Global Structure of the El Niño/Southern Oscillation Part II. Time Evolution

By Tetsuzo Yasunari*

Department of Meteorology, Florida State University, Tallahassee, FL32306
(Manuscript received 19 August 1986, in revised form 19 December 1986)

Abstract

Time evolutions of anomalies of SST and atmospheric parameters over the global domain were investigated for the several ENSO cycles during the period 1964-79, using the data set described in Part I. The principal results are summarized as follows:

1) the eastward propagation of SLP and zonal wind anomalies from the Indian Ocean toward the eastern Pacific is a fundamental nature of ENSO along the tropics and the southern subtropics.
2) the significant anomalies of SLP and circulation field which first appear over the Indian Ocean seem to originate from central Asia or Eurasia.
3) the vertical structures of these anomalies over central Asia at the intermediate stages of the cycle (*i.e.*, about one year before the SST maximum (minimum) over the equatorial Pacific) are suggested to represent large-scale cold (warm) air outbreak associated with more (less) than normal snow cover over there.
4) a time-lag teleconnection between the north Pacific and central Asia is found in the circulation field, which seems to have a key role on the mechanism of ENSO cycle.

The first two results have substantially confirmed the evidences of ENSO signals from Eurasia and the Indian Ocean toward the equatorial Pacific, which were noted in the surface fields by Barnett (1984, 1985a) and Krishnamurti *et al.* (1986).

The third result suggests the important role of Asian monsoon as a connector of the process in the extra-tropics and that in the equatorial Pacific. The fourth result seems to be associated with the interaction between the PNA and the EU (Eurasian) pattern with a time lag of half a year or more.

The links between the tropics and the extra-tropics and between the ocean and the continent described above strongly suggest that the ENSO should be understood as a global scale land (cryosphere)-atmosphere-ocean coupled system rather than an atmosphere-ocean coupled system over the equatorial Pacific.

1. Introduction

In the earlier study (Yasunari, 1987: hereafter referred to as Part I) we first demonstrated the objective analysis scheme for time-filtered station data by using the least-square method (Pan, 1979). We then investigated the global distributions of anomalies in the sea surface temperature (SST) and the atmospheric parameters for the El Niño phases by compositing the four events. The anomalies over and around the tropical Pacific region proved to be consistent with the previous observational studies (Arkin, 1982; Pan and Oort, 1983 etc.). It has also been noted that the atmospheric as well as the oceanic anomalies associated with the El Niño event are not confined within the tropical Pacific but are distributed over the global domain.

The current paper will examine the time evolution of the whole ENSO cycle (*i.e.*, from the El Niño to anti-El Niño and again from anti-El Niño to El Niño) by compositing the time-filtered anomalies of the four or five ENSO cycles. A possible physical process for the ENSO cycle will finally be discussed.

*Present Affiliation: Institute of Geoscience, University of Tsukuba, Ibaraki 305, Japan.

2. Methods

As described in section 4 of Part I, the time-filtered anomalies of SST and objectively analyzed atmospheric parameters (zonal and meridional wind, temperature, geopotential height) in the troposphere and the sea level pressure (SLP) are categorized to 8 phases for each ENSO cycle during 1964 through 1979 in reference to the smoothed Southern Oscillation Index (SOI) values. Category 1 (5) denotes the maximum (minimum) SOI phase, which corresponds to the anti-El Niño (El Niño) period. Similarly, category 3 (7) corresponds to the intermediate stage from the anti-El Niño (El Niño) to the El Niño (anti-El Niño) period. One category of each ENSO cycle has a 5 to 6 months time length. To scrutinize the circulation, temperature and height anomalies over the whole global domain associated with the ENSO cycle, composite anomaly fields for each category are produced, by averaging the four (or five) cases during the analysis period (1964–79). Longitude-time sections of the filtered data are also produced to examine the stationarity or non-stationarity of the anomalies for each ENSO cycle.

3. Evolution of SST

It has been already noted that the positive SST anomalies appear nearly simultaneously in the whole tropics except the equatorial western Pacific during the El Niño events (refer to Fig. 6 of Part I). This is clearly shown in the longitude-time section of filtered SST along the equator (Fig. 1). Although the amplitudes of anomalies in the Indian Ocean and the Atlantic are far smaller than that in the eastern Pacific, the phases of the maximum (minimum) anomalies appear nearly in phase with (or slightly lag behind) the eastern Pacific. These anomalies have been interpreted as responses to anomalous circulation associated with ENSO (Reiter, 1983). In the central through eastern Pacific, SST seems to change with a slight westward component, but this may be due to the combined effect of large amplitudes of the seasonal cycle in the eastern Pacific and the strong east-west gradient in the mean seasonal SST distribution. The actual expansion of warm SST area associated with major El Niño is mostly eastward (Gill and Rassmusson, 1983).

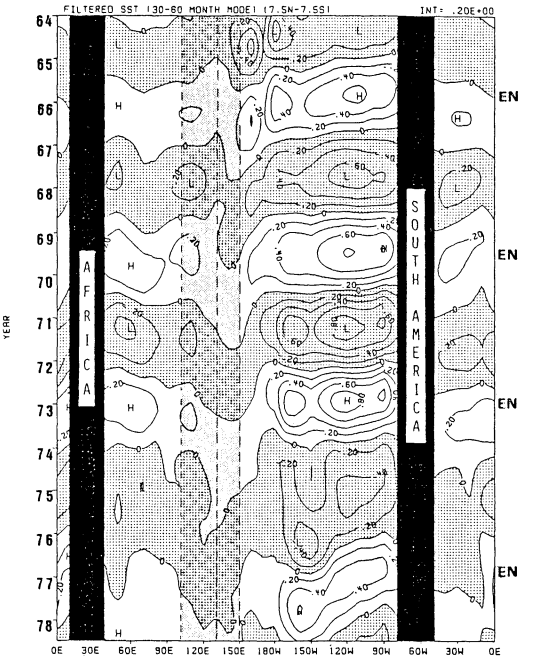

Fig. 1. Longitude time section of filtered sea surface temperature (SST) anomalies along the equator (7.5°N–7.5°S). Units are 0.2°C and negative values are shaded. Hatched area (100°E–150°E) denotes Indonesian maritime continent region. The areas of black colors denotes the continents. El Niño phases are also indicated with "EN".

The cold SST anomaly in the northern Pacific is another dominant feature during El Niño (see Fig. 6 of Part I). To examine the association of the anomalies there with those in the equatorial Pacific in time sequence, the latitude-time section of the filtered anomalies in the central Pacific (160°E–130°W) is produced (Fig. 2). A standing-type north-south oscillation is predominant in the middle and low latitudes (40°N–40°S) with out of phase relation between the equator and the northern (and the southern) mid-latitudes. This has been already noted in the earlier studies (Hsiung and Newell, 1983 etc.). It is worth noting, however, that particularly in the northern latitudes there seems to be some time lag between the maximum (minimum) SST in the equator and the minimum (maximum) SST in the mid-latitudes (30°N–40°N) with one season or so. The positive correlation between

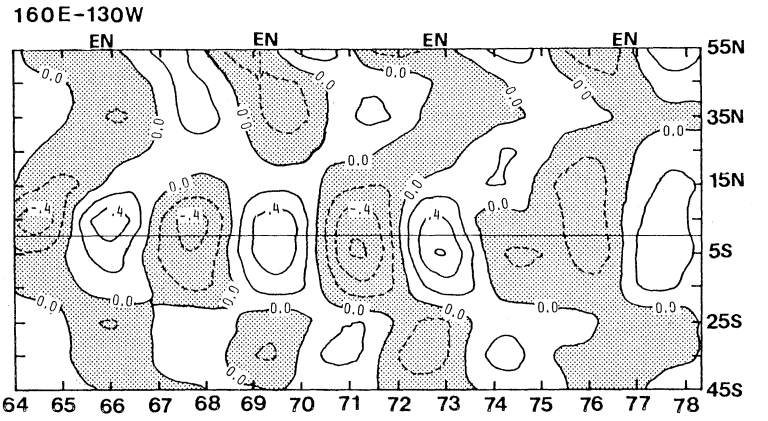

Fig. 2. Latitude time section of filtered SST anomalies along central Pacific (160°E–130°W). Units are 0.2°C and negative values are shaded. El Niño phases are also shown with "EN".

the northern high latitudes (50°N–60°N) and the equator with a phase lag of about one year is also noticeable.

The anomalies at mid-latitudes have been postulated as a result of atmospheric anomalies which may be a response of the equatorial heating anomalies (Newell *et al.*, 1982). The anomalies at higher latitudes (50°N–60°N) may be related to warmer (colder) air advection associated with more cyclonic (anticyclonic) condition at mid-latitudes, as Niebauer (1986) pointed out. He showed that the maximum SST minimum sea ice and maximum air temperature over Bering Sea lag the minimum SOI with 3 to 4 seasons. The anomalies at higher latitudes (50°N–60°N) in Fig. 2 are consistent with his results. Thus, the SST anomalies in the northern Pacific seem to be fundamentally explained by the atmospheric anomalies produced as a linear response of the equatorial anomalous heating. However, a positive feedback of SST anomalies to circulation anomalies is also possible over the north Pacific (Reiter, 1983). We also notice a slow northward propagation of the anomalies from the equator to the mid-latitudes and a southward propagation from the subpolar latitudes to the mid-latitudes. These evidences may suggest that a slow advective process in the ocean surface layer *via* the subtropical and the subpolar gyre is partly responsible for the SST anomalies in the northern Pacific (Reiter, 1978; Kawamura, 1986).

In the western Pacific region (120°E–150°E), the fluctuation of the SST anomalies in the latitude-time domain (Fig. 3) appears to be quite different from that in the central Pacific (Fig. 2). Although the anomalies at the equator are very small compared to the eastern Pacific, those in

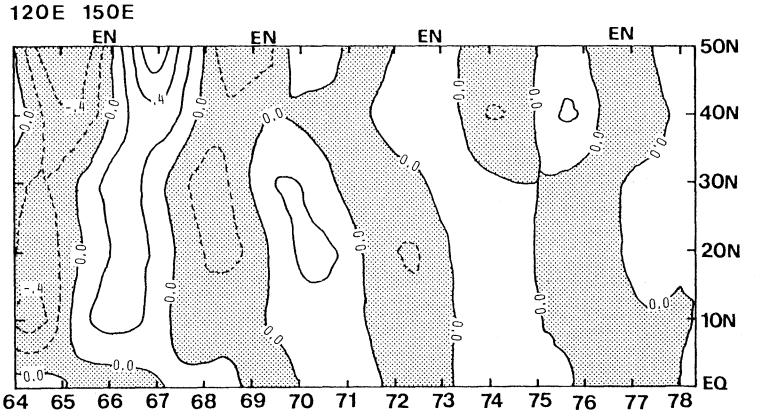

Fig. 3. Same as Fig. 2 but for the western Pacific (120°E–150°E).

the subtropics (20°N–40°N) are considerably large. It is worth noting that the phases of maximum (or minimum) in the subtropics seem to be in quadrature with those at the equatorial eastern Pacific. That is, the maximum anomalies there seem to lag behind the El Niño (the maximum in the equatorial eastern Pacific) with about a half or one year. If we note the atmospheric process, a diminished cloud amount over there associated with El Niño condition in the western Pacific may account for the high SST (Newell *et al.*, 1982). If we note the oceanic process, the slow advection of warm water in the mixed layer *via* the north equatorial current may be more important. Along this line Yamagata *et al.* (1985) showed some evidences of lagged relation between the Kuroshio extension and the north equatorial current. In any case, further study is needed for this problem.

4. Evolution of atmospheric anomalies

a. SLP

Since Walker and Bliss (1932), SLP has been one of the important parameters relevant to the Southern Oscillation (SO). Recently, Barnett (1985) and Krishnamurti *et al.* (1986) independently examined the time-evolution of SLP anomalies associated with the SO over the global domain, by utilizing different data sets and methods. Although their emphasis points are somewhat different each other, they both claimed the significantly large anomalies outside the SO region in a narrow sense (*i.e.*, the Pacific through the Indian Ocean in the tropics), which precede the extreme phases of the ENSO over the equatorial eastern Pacific. Particularly, the appearance of anomalies in the extratropics of the northern and/or the southern mid-latitudes in the Indian Ocean sector and the eastward propagation of these anomalies toward the Pacific basin is a prominent common feature noted in these two papers. Here, we re-examine the global evolution of SLP anomalies associated with the ENSO cycle.

Fig. 4 shows the composite SLP anomalies from category 1 to category 5. As mentioned in Part I, category 1 denotes the maximum SOI (anti-El Niño) phase and category 5 denotes the minimum SOI (El Niño) phase, respectively. At category 1 the anomalies relevant to the SO (*i.e.*, positive anomalies over Australia and negative anomalies over the eastern Pacific) is dominated in the low latitudes. East- or southeast-ward extension of negative anomalies from Australia to the southern Pacific may correspond to more than normal cumulus convection along the ITCZ in the western Pacific and SPCZ. The area of positive anomalies in the eastern Pacific is nearly identical with that of the cold SST anomalies. In the northern extratropics, the large north-south anomaly contrast is significant over the western Europe through the Atlantic. This may be closely related to the North Atlantic Oscillation (NAO) as described in Part I. In the southern extratropics, the positive anomalies over the southwestern Pacific and the southern Atlantic near Antarctica are noted. Since the anomalies described here are not normalized, the amplitudes are generally large in the extratropics than in the tropics. At category 2 the overall feature is similar to that at category 1, but the east-west anomaly contrast between Australia and the equatorial eastern Pacific are considerably diminished.

At category 3, which corresponds to the intermediate stage from anti-El Niño to El Niño phase, some drastic changes are apparent especially over Eurasia and the Pacific region. The east-west anomaly contrast over Australia and the eastern Pacific are completely diminished while the large positive anomaly area appear over Eurasia and the tropical Indian Ocean. In the northern high latitudes the anomalies are generally reversed from negative to positive values. In the southern extratropics, the negative anomalies over the Pacific subtropics and mid-latitudes and the small positive anomalies to the south of Australia should be noted, which suggest an "infant stage" of the typical weak SO (or El Niño) phase. At category 4, which roughly correspond to a half year before the mature El Niño phase, the positive anomalies over Eurasia through the Indian Ocean seem to expand toward Australia, and at the same time the negative anomalies are developed over the eastern south Pacific. At this stage, the north-south SLP contrast over the Atlantic through western Europe is reversed in sign. If we refer to the composite SST anomaly maps (not shown here), warm SST anomalies are widely developed over the equato-

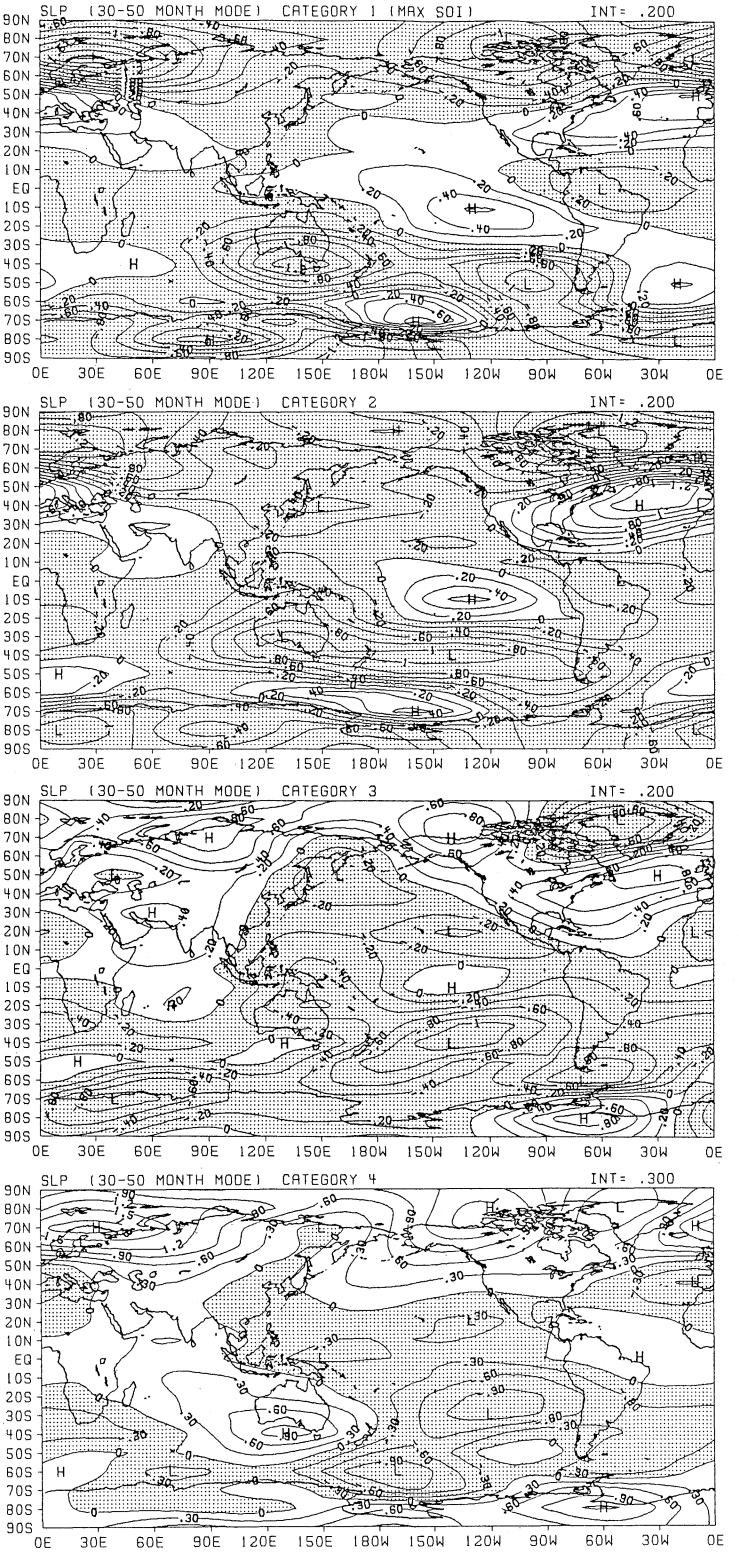

Fig. 4. Composite filtered anomalies of SLP for category 1 to 4. Units are indicated on the right up side of each diagram. Negative values are shaded.

rial central and eastern Pacific. At category 5 (El Niño phase) the overall anomaly pattern becomes nearly identical to the pattern of category 1, but reversed in sign.

Thus, the anomalies at category 3 and 4 strongly suggest that the El Niño signals first appear over Eurasia through the Indian Ocean about one year before the extreme event over the eastern Pacific. Surprisingly, the overall pattern at category 3 and 4 are very similar to the anomaly patterns of a half- and one-year before the El Niño of 1972 and 82 produced by Barnett (1985). (Note that one category roughly denotes half a year as mentioned in Part I), the small positive anomalies to the south of Australia at category 3 develop and expand rapidly over Australia through category 4 and 5. This feature may agree with the result by van Loon and Shea (1985), where they noted this phenomenon as a precursor to the El Niño.

Fig. 5 shows the longitude-time section of the composite anomalies of the whole ENSO cycle (category 1 to 8) for the northern and the southern subtropics. The SO has been recognized as a standing-type oscillation along the southern subtropics (Troup, 1965; Kidson, 1975 etc.). However, these diagrams show that the eastward propagation of anomalies from the Indian Ocean to the Pacific is a salient feature in the southern subtropics, while the standing-type oscillation be-

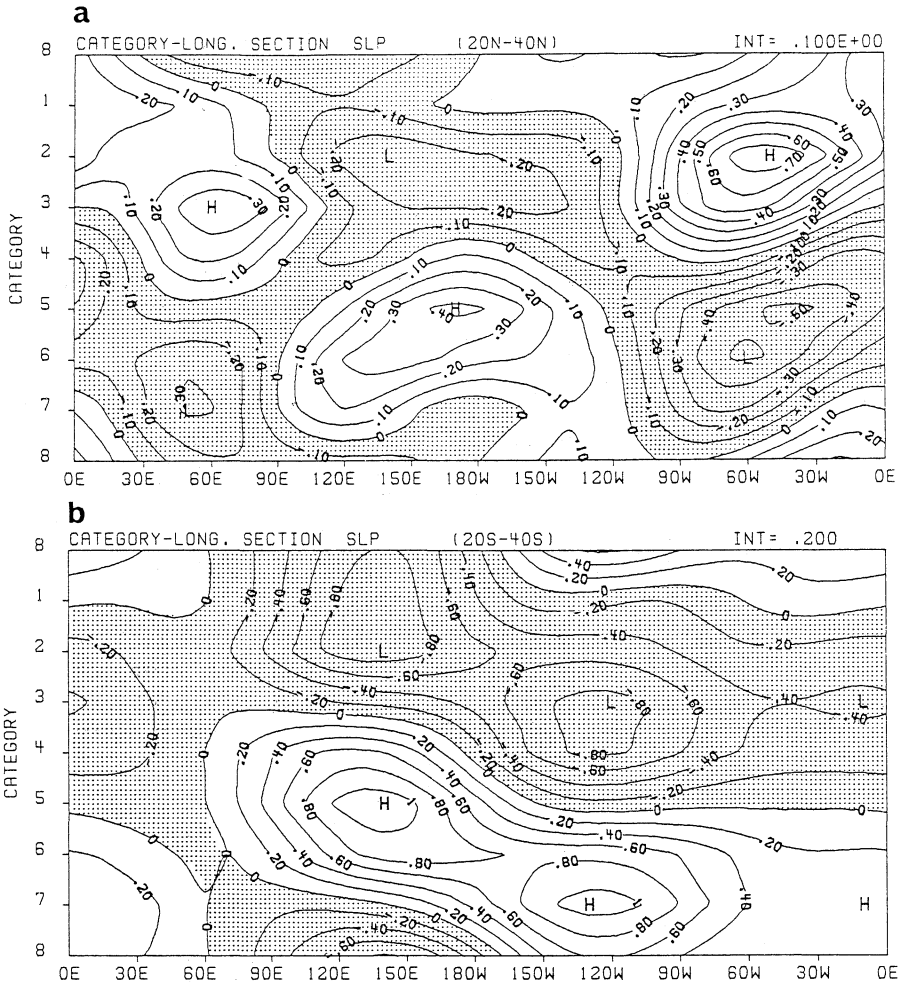

Fig. 5. Longitude-category section of filtered SLP anomalies for (a) northern subtropics (20°N–40°N) and (b) southern subtropics (20°S–40°S). Units (mb) are shown on the right up. Negative values are shaded.

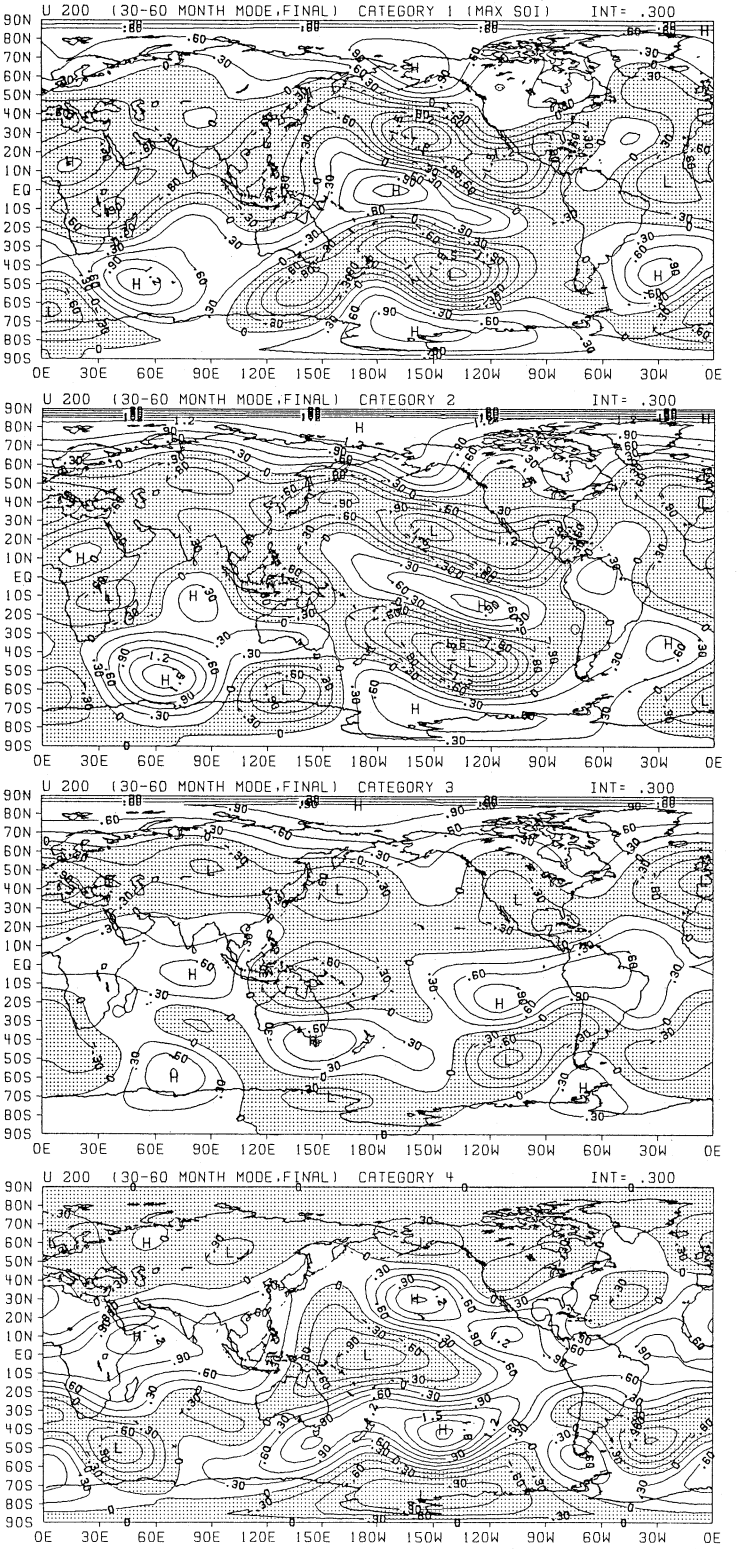

Fig. 6. Same as Fig. 4 but for zonal wind at 200 mb. Units are 0.3 m s^{-1}.

tween the Eurasia-Atlantic region and the Pacific region is prominent in the northern subtropics.

b. zonal wind

It has been elucidated that the zonal wind anomalies associated with the ENSO considerably change in the subtropics and mid-latitudes (refer to Fig. 8 and 10 in Part I) as well as in the tropics (Barnett, 1984; Yasunari, 1985 etc.).

Fig. 6 shows the composite zonal wind anomalies at 200 mb from category 1 to category 4. Category 5 (El Niño phase) is nearly the same as category 1 but with opposite sign (refer to Fig. 6 of Part I). At category 1 (anti-El Niño phase) easterly anomalies are dominated in the tropics and mid-latitudes except the equatorial central Pacific, while the westerly anomalies are dominant in the high latitudes. Along the equator, a stronger than normal east-west circulation is suggested with the upward portion over the Indonesian maritime continent and the downward portion over the eastern Pacific. Only a slight change of pattern is seen at category 2. The westerly anomalies over the central Pacific seem to be shifted slightly eastward.

At category 3 the anomaly pattern seems to be changed considerably from category 2. The appearance of westerly anomalies over the tropical Indian Ocean is noticeable. The westerly anomalies over the eastern Pacific is further shifted eastward and is extended over south America. In the mid-latitudes the easterly anomalies over the northern and the southern Pacific are reduced. At category 4 the anomaly pattern

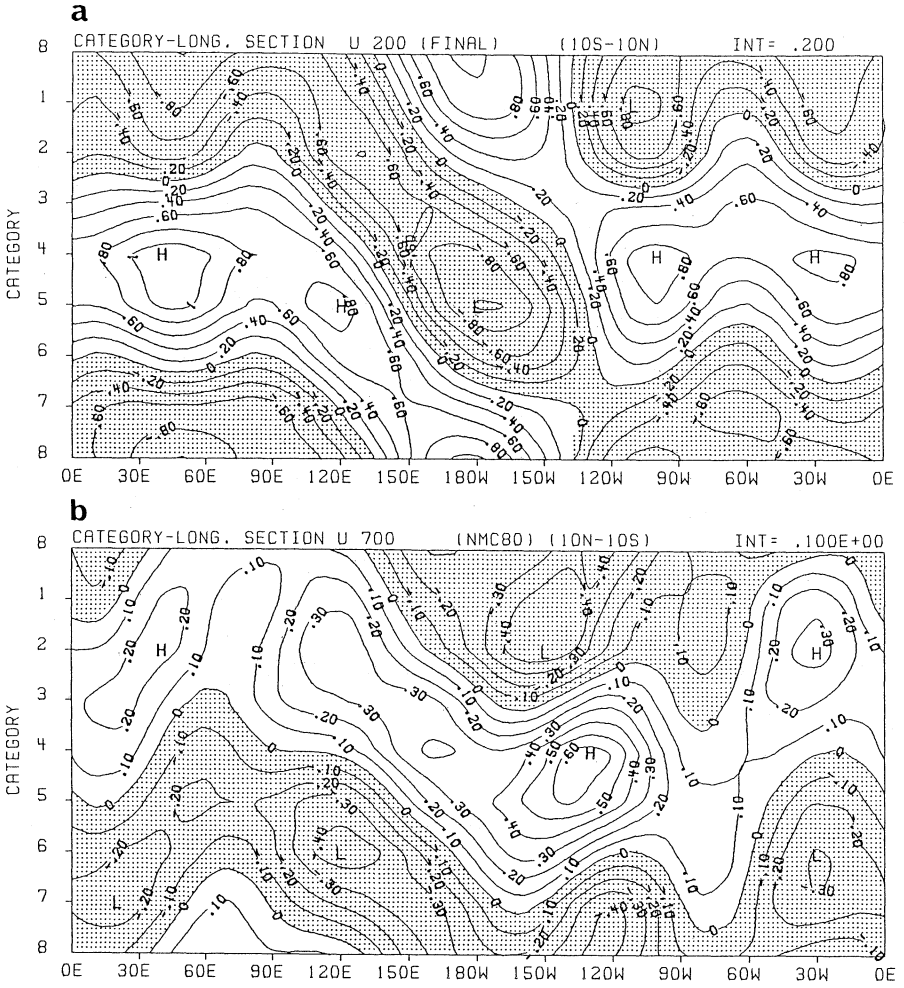

Fig. 7. Same as Fig. 5 but for zonal wind at 200 mb. Units are shown on the right up. Negative values are shaded.

over the whole globe is completely changed to the El Niño pattern (Fig. 8 of Part I). The westerly anomalies are now dominated over the tropics and the mid-latitudes, and the westerlies in the polar latitudes at category 1 to 3 are replaced with the easterlies.

The eastward propagation of zonal wind anomalies in the upper and the lower troposphere along the equatorial belt noted by Yasunari (1985) is confirmed in the longitude-time section of the composite anomalies as shown in Fig. 7. The anomalies at 200 mb and 700 mb particularly over the Indian Ocean through the central Pacific consist of the upper and lower part of the anomalous east-west circulation along the equatorial plain. The eastward propagation of these cells (*e.g.*, note the zero lines between the easterlies and the westerlies at 200 mb) are nearly consistent with the eastward propagation of SLP anomalies in the southern low latitudes (Fig. 5 (b)).

To examine whether the vertical structure of anomalies is equivalent barotropic or baroclinic, the correlation coefficients of zonal wind anomalies between 200 mb and 700 mb are computed for every 10° lat. × 30° long. blocked area (Fig. 8). As postulated from Fig. 8, a baroclinic-type structure (negative correlation) is dominant along the equatorial belt over the Indian Ocean through the central Pacific. It is noteworthy that even in the tropics baroclinic-type response is not apparent over south America through the Atlantic. This may suggest that the anomalous diabatic heating responsible for the ENSO is confined over the Indian Ocean through the Pacific. The negative correlations, though not so significant, over the northern Atlantic may be related to large variability of the upper westerly jet associated with the activity of baroclinic disturbances. The reason for negative correlations over the southern Indian Ocean is not clear. In other parts of the world positive correlations (equivalent barotropic-type anomalies) are dominated.

Since the anomalous heating in the tropics during the El Niño is so global as shown in Fig. 11 of Part I, the zonal mean wind change should be considerably large associated with the ENSO cycle. Actually, Rosen *et al.* (1984) found that the total atmospheric angular momentum and length of day increased during 1982/83 El Niño. If we refer to the global distribution of zonal wind anomalies (see Fig. 6), we can postulate that the general increase of westerly anomaly in the lower latitudes may contribute the increase of total westerly angular momentum of the atmosphere. Fig. 9 shows longitude time section of zonal mean wind at 200 mb and 700 mb. A prominent feature is a poleward propagation of anomalies, particularly in the northern hemisphere. The westerly (easterly) maximum in the lower latitudes (centered in the subtropics) nearly correspond with the El Niño (anti-El Niño) phase. The westerly (easterly) anomalies at 200 mb and 700 mb are nearly in phase each other except around the equator. This may imply the barotropic-type response of the global atmosphere as a whole to the anomalous heating in the tropics. From these diagrams we easily speculate the increase (decrease) of the total atmospheric angular momentum during El Niño (anti-El Niño) as Rosen *et al.* (1984) suggested. It is noteworthy

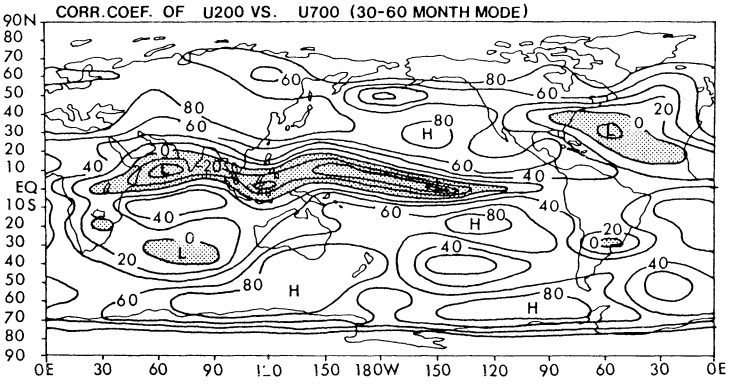

Fig. 8. Distribution of correlation coefficients between U at 200 mb and U at 700 mb. Units are 0.2 (multiplied by 10^2). Negative values are shaded.

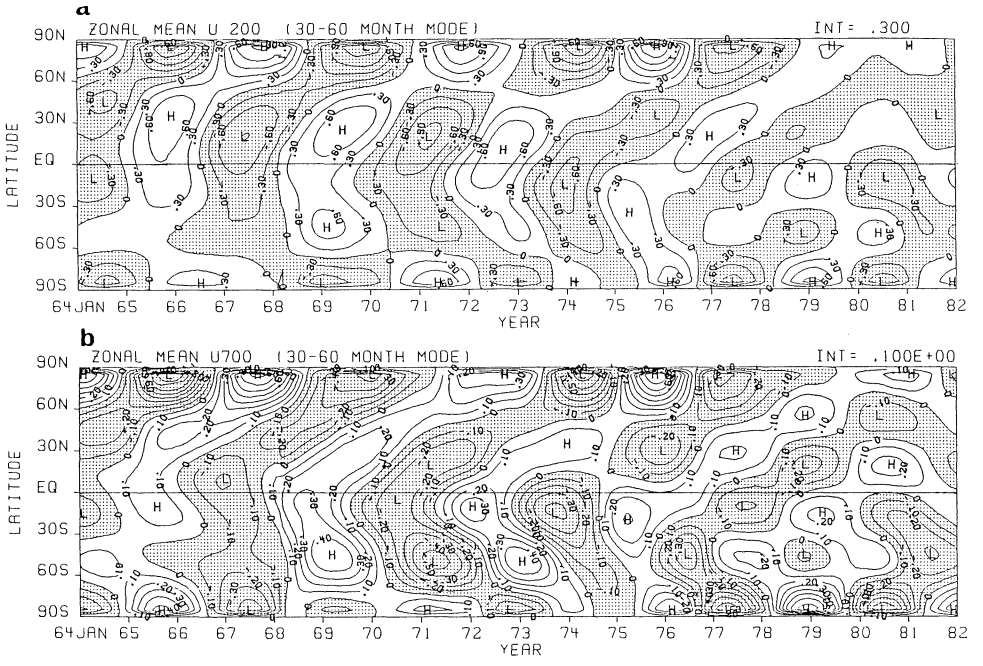

Fig. 9. Latitude time section of zonally averaged zonal wind anomalies for (a) 200 mb and (b) 700 mb. Units (m s^{-1}) are indicated on the right up. Negative values are shaded.

that the phase speed of poleward propagation is different each other in the northern and the southern hemisphere. This may be partly due to the difference of accuracy of data between the northern and southern hemisphere but most probably due to the difference of response process in each hemisphere.

c. temperature

The temperature anomaly associated with the ENSO appears most significantly in the upper troposphere (Pan and Oort, 1983). Fig. 10 shows composite temperature anomalies at 300 mb from category 1 to category 4. Category 5 (El Niño phase) is shown in Fig. 11 (a) of Part I. At category 1 (anti-El Niño phase) and 2 negative anomalies are predominant in the tropics with the minimum over the central Pacific, while positive anomalies are distributed along mid-latitudes. At category 3 the positive anomalies at mid-latitudes are diminished particularly in the northern hemisphere. Negative anomalies seem to be intensified over south and central Asia. At category 4, about half a year before the mature El Niño phase (category 5), anti-El Niño pattern has completely disappeared. The negative anomalies over south and central Asia further developed, while positive anomalies have rapidly evolved over the central Pacific region. At category 5 positive anomalies are extended over the whole tropical belt with the maximum over the equatorial central Pacific, while negative anomalies are elongated along mid-latitudes as described in Part I. The large negative anomalies over south and central Asia developed at categories 3 and 4 may presumably be associated with strong cold air outbreak in winter and/or weak monsoon in summer which precede the El Niño event over the equatorial Pacific. We will discuss further about this problem.

d. circulations

Finally, the global non-divergent and divergent circulation changes during the ENSO cycle are described by using streamfunction and velocity potential anomalies computed from U and V anomalies. Fig. 11 (a) shows the composite streamfunction (Ψ) field at 200 mb from category 1 to 4. At category 1 (anti-El Niño phase) anticyclonic conditions are dominant at high and middle latitudes of the two hemispheres, which are consistent with the easterly

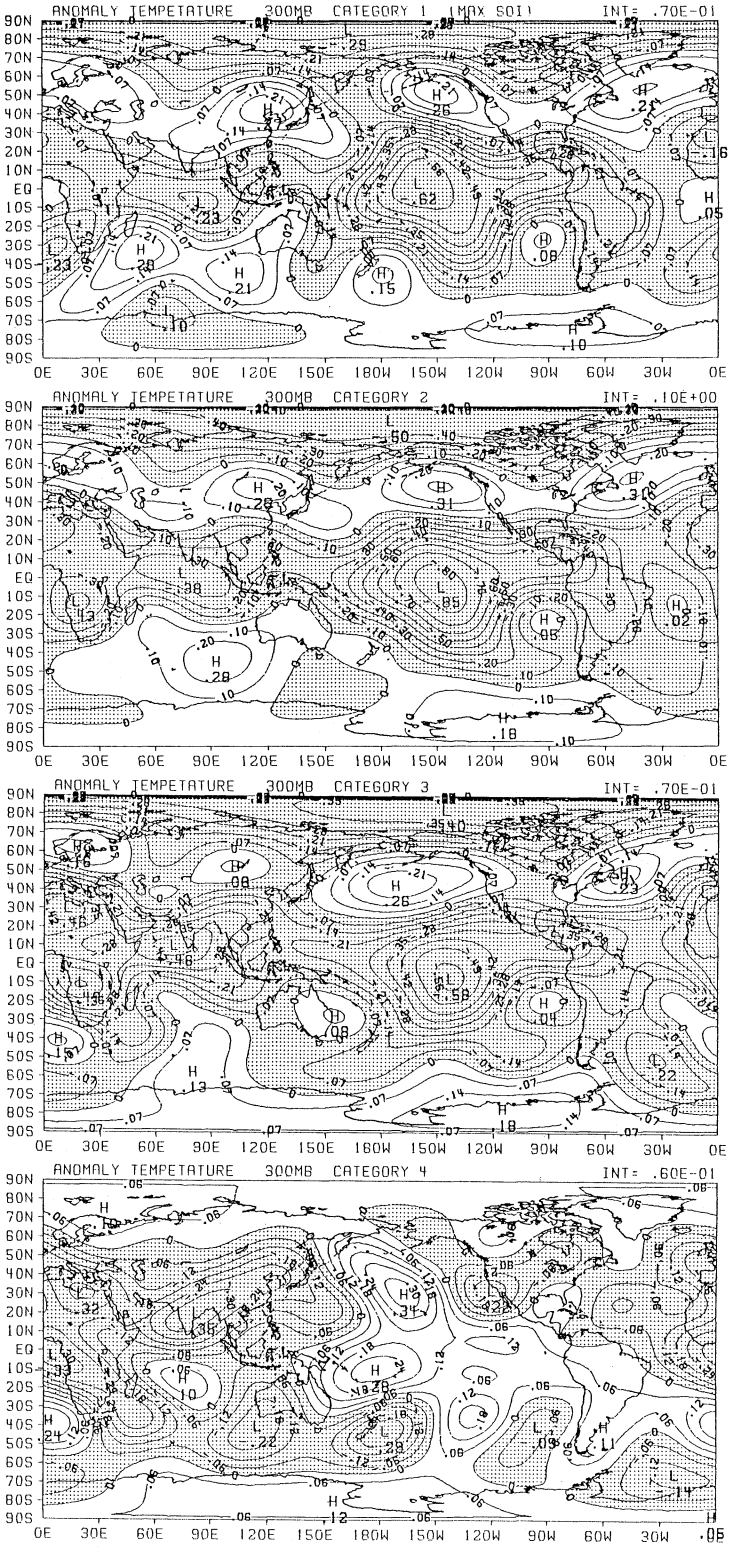

Fig. 10. Same as Fig. 4 but for temperature at 300 mb. Units (°C) are indicated on the right up. Negative values are shaded.

(a)

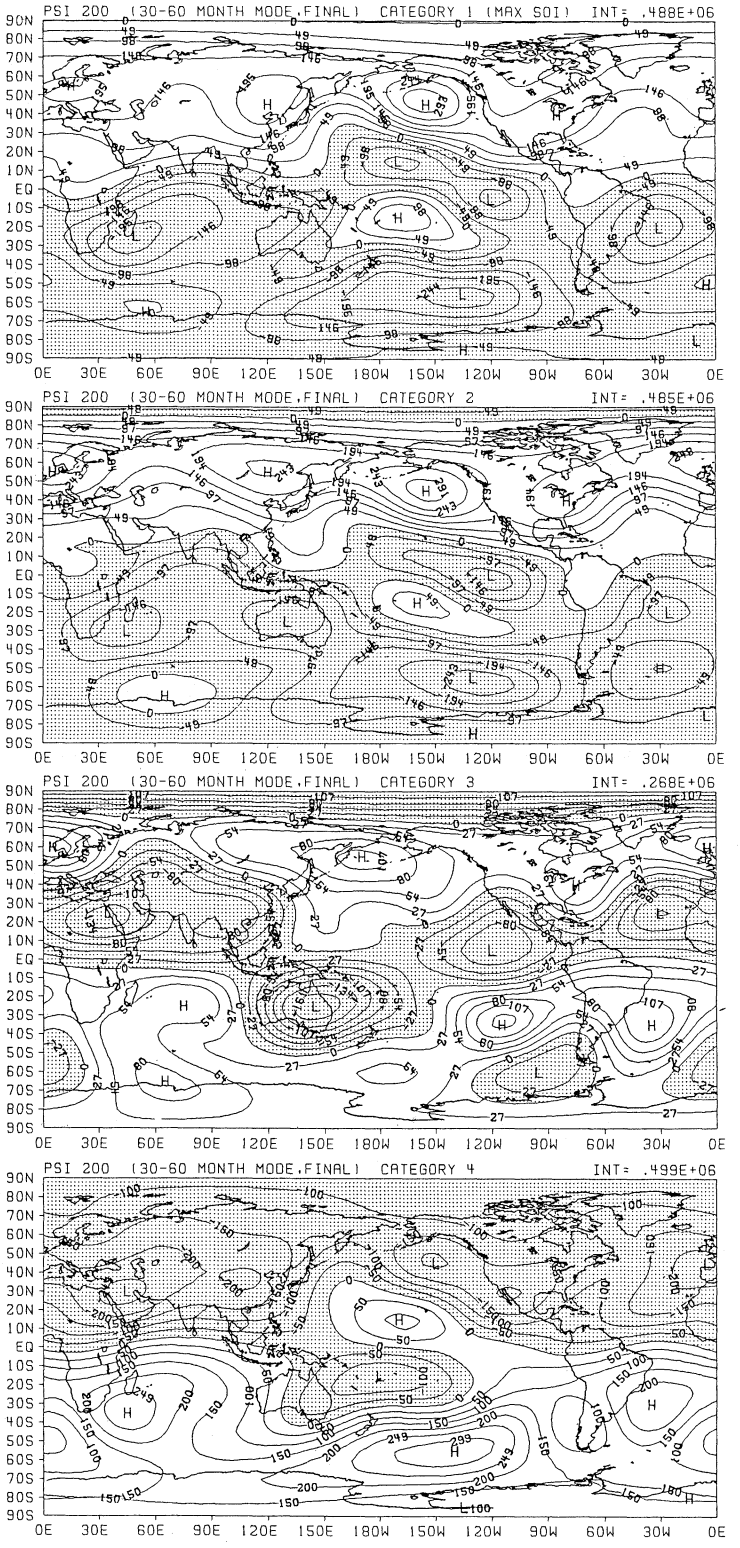
PSI 200 (30-60 MONTH MODE,FINAL) CATEGORY 1 (MAX SOI) INT= .488E+06
PSI 200 (30-60 MONTH MODE,FINAL) CATEGORY 2 INT= .485E+06
PSI 200 (30-60 MONTH MODE,FINAL) CATEGORY 3 INT= .268E+06
PSI 200 (30-60 MONTH MODE,FINAL) CATEGORY 4 INT= .499E+06
90N 80N 70N 60N 50N 40N 30N 20N 10N EQ 10S 20S 30S 40S 50S 60S 70S 80S 90S
0E 30E 60E 90E 120E 150E 180W 150W 120W 90W 60W 30W 0E

(b)

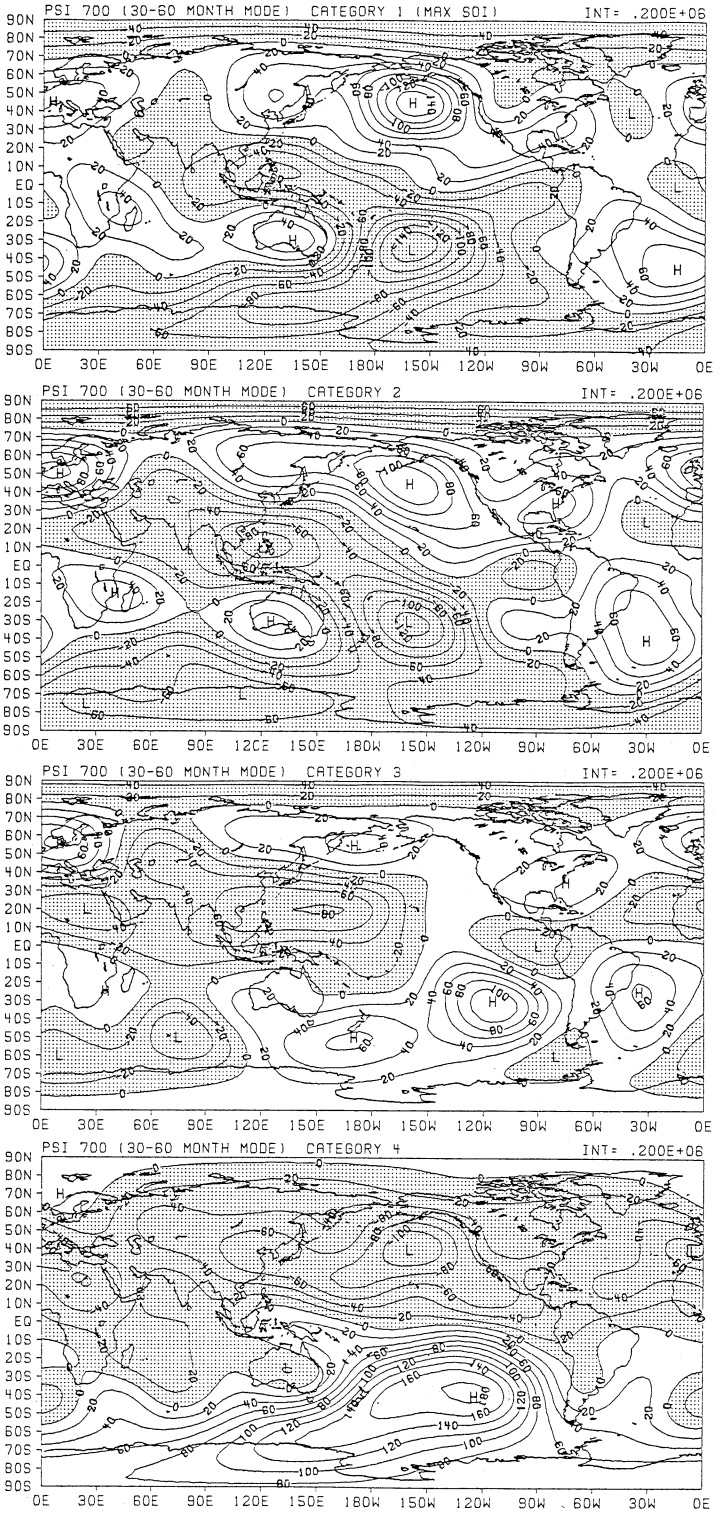

Fig. 11. Same as Fig. 4 but for streamfunction at (a) 200 mb and (b) 700 mb. Units ($m^2\ s^{-1}$) are shown on the right up. Negative values are shaded. Note that L and H denotes center of cyclonic (anticyclonic) and anticyclonic (cyclonic) circulation in the northern (southern) hemisphere.

anomalies over there as shown in Fig. 6. In the Pacific region double cyclonic anomalies (L in the northern Pacific and H in the southern Pacific) spread to the north and the south of the equator and anticyclonic anomalies polewards are salient features. Over the north Pacific a reversed PNA pattern is noted. Along the equator, easterly anomalies over the Indian Ocean and the westerly anomalies over the central Pacific are noticeable. At category 2 the overall feature is very similar to category 1.

A drastic change of the anomaly Ψ field is noticed again at category 3 as well as SLP field (Fig. 4). The meridionally-oriented wave-like structure over the Pacific noted at category 1 and 2 are completely diminished. In the southern low latitudes a strong anticyclonic cell appear over Australia, while cyclonic cells appear over the eastern Pacific, the Atlantic and the Indian Ocean. In the northern low latitudes a cyclonic circulation is intensified especially over north Africa through southern Eurasia. At category 4 and 5 the overall feature is analogous to that of category 1 or 2 but with the opposite sign. At category 5 (El Niño phase) a double anticyclonic cell structure over the equatorial central Pacific and PNA pattern are explicitly shown.

In the lower troposphere (700 mb) the anomalous Ψ field (Fig. 11 (b)) seems to be similar to that at 200 mb in most parts of high and middle latitudes, but in most parts of tropics the pattern seems to be similar but with opposite in sign. At category 1 and 2, the anticyclonic circulation is dominant over the northern Pacific, which is barotropically consistent with that at 200 mb. In the southern low latitudes, the cyclonic circulation over Australia and the anticyclonic circulation over the central Pacific is noticeable, which is consistent with the SLP anomalies (Fig. 4). The twin cyclonic cell structure is also apparent over the Indonesian maritime continent, which may represent stationary Rossby-wave response to heat source over there (Matsuno, 1966, Gill, 1980).

At category 3, the overall circulation pattern changes considerably over the entire Pacific domain. In the northern Pacific anticyclonic anomalies over the Aleutian Low area is weakened and alternately, the cyclonic anomalies spread eastward over the whole northern Pacific region from the Asian continent. In the southern hemisphere, the east-west contrast of circulation anomalies over Australia through the Pacific has completely disappeared. Instead, a cyclonic anomalies appeared over the eastern Pacific, which implies the weakening of the south Pacific high and/or the equatorward extent of mid-latitude westerly trough. It is noteworthy to state that at this stage the anomalous westerlies are dominated over the entire equatorial Pacific. At category 4, the cyclonic anomalies over the southern Pacific furthern developed and the anticyclonic anomalies appeared over Australia, which nearly correspond to the pattern at El Niño phase.

Fig. 12 shows the composite anomalies of velocity potential (X) at 700 mb from category 1 to 4. Here, X is defined as such that minimum values denote centers of convergence. At category 1 (anti-El Niño phase) a center of convergence is located over the Indonesian maritime continent and a center of divergence is located over the equatorial eastern Pacific. Another center of convergence and diverdgence is located over north Africa and over the Caribbean Sea respectively, which may consist of another east-west circulation cell over the Atlantic. The overall feature shows a wavenumber-one structure, which suggests the east-west (or Walker) circulation along the equatorial Pacific is a dominant divergent circulation over the globe. At category 2 the overall pattern resemble with that of category 1, but the center of convergence over Indonesia seems to be slightly shifted eastward and a small center of divergence appear over the Indian Ocean.

A drastic change occurs again at category 3. The center of divergence over the Indian Ocean develops and is extended over the eastern hemisphere while the center of convergence over the maritime continent is shifted further eastward and is replaced with the center of divergence over the central Pacific. That is, the wavenumber-one structure is reversed in sign. At category 4 and 5 (El Niño phase) the total feature is fundamentally the same as category 3, but the main centers of divergence and convergence seem to be moved further to the east, (*i.e.*, over the maritime continent and the eastern Pacific).

At 200 mb (not shown) the anomaly patterns

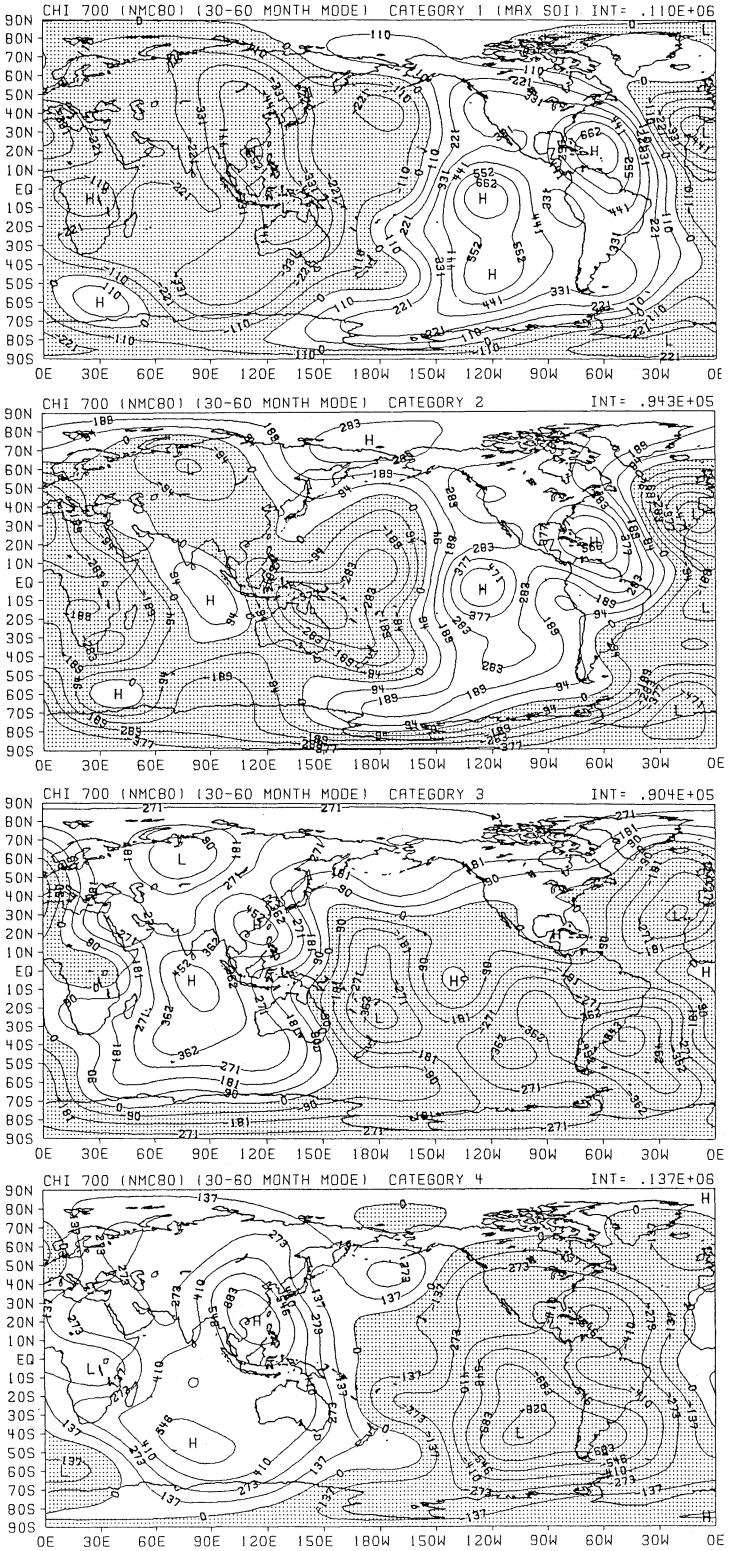

Fig. 12. Same as Fig. 4 but for velocity potential at 700 mb. Units (m^2 s^{-1}) are indicated on the right up. Negative values (convergence) are shaded.

of velocity potential particularly over the tropics are roughly consistent with those at 700 mb with an opposite sign. However, unfortunately, the global patterns seem to be considerably distorted because of large errors in divergent wind field over the southern middle and high latitudes.

5. Mechanism of evolution

a. process in the tropics

Some remarkable features have been noted in the time evolutions of global SST and atmospheric anomalies associated with the ENSO cycle.

The eastward propagations of some atmospheric parameters (SLP, zonal wind, velocity potential) along the equator and the southern subtropics have been confirmed as most prominent aspects of ENSO in the low latitudes. As described in Yasunari (1985), this phenomenon is characterized as a zonally propagating mode of the tropical east-west (or Walker) circulation, though the standing mode also occupies a considerable portion of variance (Barnett, 1985b). This eastward propagation in the wind field has also been noted recently by Gutzler and Harrison (1986). In addition, the present results suggest that this eastward propagation in the tropics is coupled with the eastward propagation of SLP anomalies in the southern subtropics.

It should be emphasized here that the significant changes of anomalies in SST and atmospheric anomalies appear at the intermediate stage from anti-El Niño to El Niño (*i.e.*, category 3) or *vice versa* (*i.e.*, category 7). As has been noted earlier, at category 3 the upper level anticyclonic anomalies over Australia is considerably intensified and slightly shifts eastward (refer to Fig. 11 (a)), while at the surface the negative SLP anomalies are extended from northeast Australia southeastward along SPCZ. Simultaneously, the south Pacific high is considerably weakened (Fig. 4). At 700 mb the center of convergence moves further eastward from northern Australia and the westerly anomalies are extended eastward along the equator. These features totally suggest that the center of convection over the western Pacific has moved eastward from its normal position. As has been pointed out by many authors (Luther *et al.*, 1983 etc.), this situation over the equatorial western through central Pacific is a necessary, or otherwise, favourable condition for triggering the El Niño.

Once the trade wind over the central Pacific is weakened, or the equatorial westerlies over the western Pacific is intensified associated with this situation, some sort of unstable atmosphere/ocean interaction (*e.g.*, by Philander *et al.* (1984)) may trigger eastward propagation of anomalies.

What, then, causes the eastward shift of convection and wind field? van Loon and Shea (1985; 1987) emphasized the role of SPCZ and the mid-latitude circulation in the Australia-south Pacific sector. However, our analysis strongly suggests that the preceding ENSO signals come further from the west, *i.e.*, the Indian Ocean side. The scenario by van Loon and Shea may possibly be a part of our scenario if we include the downstream effect of atmospheric process over the southern Indian Ocean.

b. process over Eurasia and Indian Ocean

The positive SLP anomalies, negative temperature and streamfunction anomalies in the upper troposphere and the positive (divergent) anomalies of velocity potential at 700 mb over Eurasia and the northern Indian Ocean at category 3 suggest us, as a whole, that the cold air out-break associated with the southward extended trough over this region about one year before the mature El Niño phase may have a key role to the phase change from anti-El Niño to El Niño condition.

Here, we should recall the negative correlation between the Eurasian snow cover extent and the following Indian monsoon rainfall amount pointed out first by Blanford (1884) and recently re-examined with satellite data by Hahn and Shukla (1976), Dey and Banu Kumar (1981) and Dickson (1984). The anomalies over southern Eurasia at category 3 mentioned above should be responsible for more than normal snow cover over there. To confirm this inference, composite snow cover anomalies for category 3 and 7 are produced as shown in Fig. 13. At category 3 a positive anomaly area is largely extended over Euarasia with the maximum over Tibet. Interestingly, negative anomalies are noticeable over north America. In the streamfunction anomalies (Fig. 11) cyclonic and anti-cyclonic circulation anomalies exist over the west coast and the east coast of north America, respectively. Since a

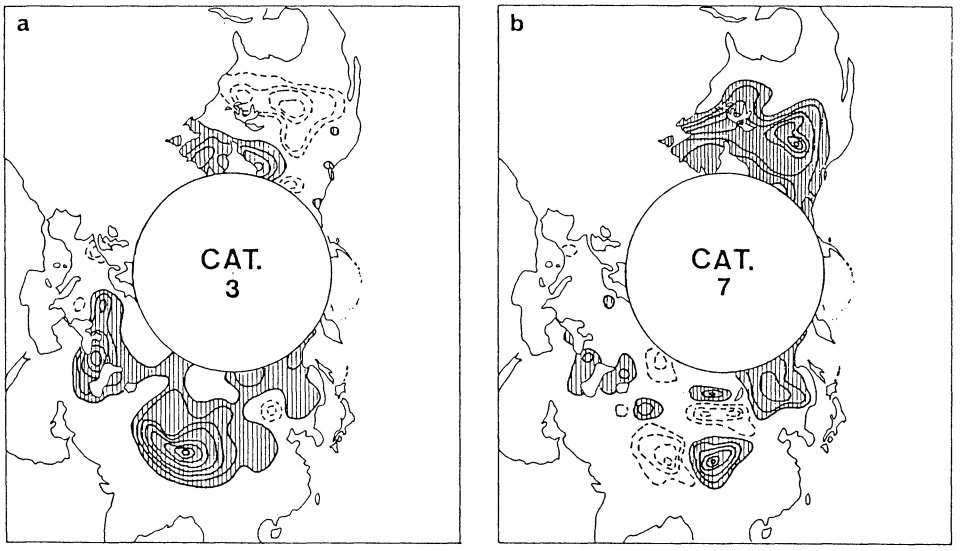

Fig. 13. Composite snow cover anomalies for (a) category 3 and (b) category 7. Unit of contour is 0.2 (Full cover of each grid is 9.0). Negative values (of less than −0.2) are shown with dotted lines, and positive values (of more than 0.2) are shaded.

stationary ridge (trough) is located over the Rockies (west coast) in a mean state, this anomaly pattern implies a more zonal flow over north America, which may be responsible for the less snow cover over there. At category 7, the anomalous condition is nearly the opposite to that at category 3, that is, less than normal snow cover over south Asia and more than normal snow cover over north America. At category 4 (and 3) the atmospheric anomalies over south Asia (*i.e.*, positive SLP, positive U at 200 mb, negative U at 700 mb, negative T at 300 mb, negative Ψ at 200 mb and positive X at 700 mb) totally characterize the weak summer monsoon condition. That is, the cold-surge type anomalies over central and south Asia with more than normal snow cover extent in cold seasons and the weak monsoon over south Asia in the following summers seem to be distinct signals prior to the El Niño events in the equatorial eastern Pacific in the following autumn and winters. These results have fundamentally confirmed the evidences of the preceding ENSO signals in SLP anomalies from Eurasia and the Indian Ocean toward the equatorial Pacific, first noted by Barnett (1985). Shukla and Paolino (1983) also noted that the anomalous summer monsoon precedes the extreme phase of ENSO in autumn through winter. In other words, the two factors, *i.e.*, the ENSO indices (SOI or SST in the equatorial Pacific) and the snow cover over Eurasia and Tibet, which are highly or moderately correlated with the Indian summer monsoon rainfall (Pant and Parthasarathy, 1981; Bhalme and Jadhav, 1984; Hahn and Shukla, 1976; Dickson, 1984 etc.) should be inferred as parts of one climate system of global ENSO rather than independent external parameters.

c. a time-lag teleconnection

As scrutinized above, there seem to be two centers of actions in the northern mid-latitudes associated with ENSO. One is the northern Pacific area where distinct anomalies appear during the extreme phases (category 1 or 5) of ENSO cycle. These anomalies have been noted in many previous studies (Horel and Wallace, 1981; Chen, 1982 etc.). The other may be central Asia or Eurasia at around 60° E, where significant anomalies appear during the intermediate phases (category 3 or 7) as noted here. The problem may be, then, how the significant anomalies of these two areas evolve and inter-relate each other during the course of ENSO cycle. To approach this problem, the longitude-category section of composite streamfunction anomalies along 40°−60°N are produced as shown in Fig. 14. Large anomalies are noticeable over central

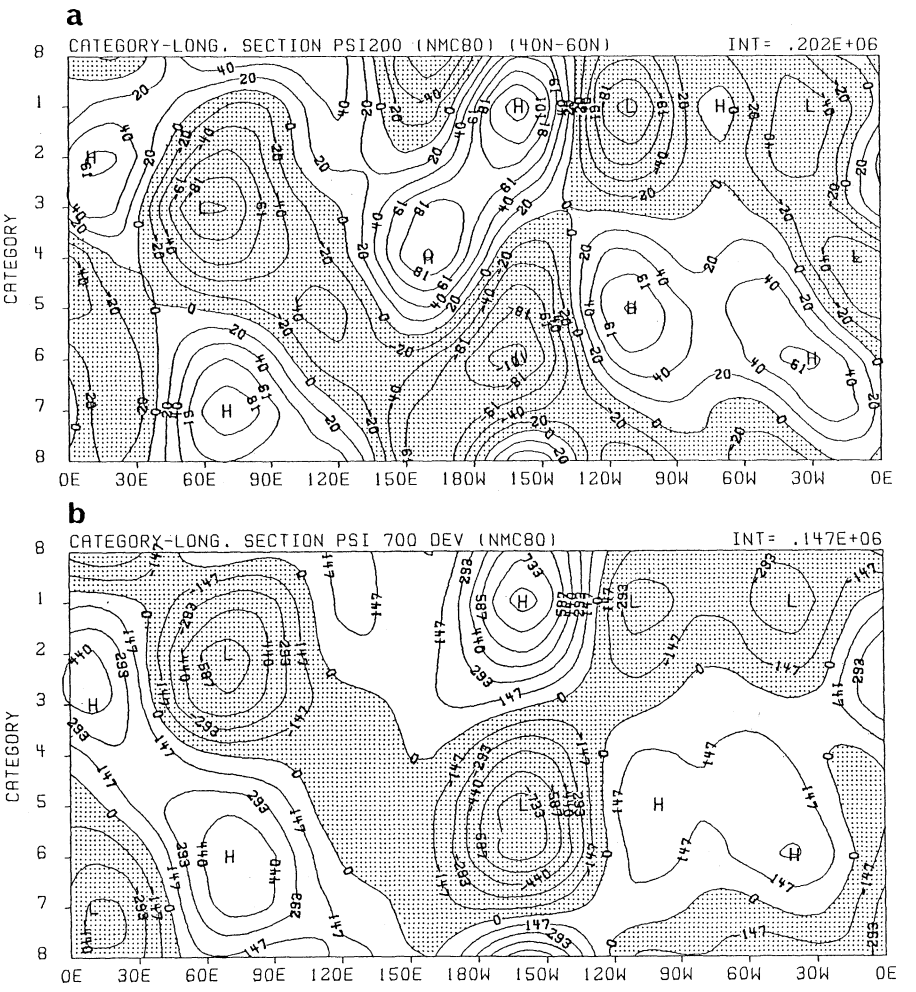

Fig. 14. Same as Fig. 5 but for (a) streamfunction at 200 mb and (b) streamfunction at 700 mb along 40°N–60°N. Zonally averaged values are subtracted. Units are indicated on the right up, and negative values are shaded.

Eurasia and northern Pacific but with one or two category lags. Particularly at 700 mb (Fig. 14 (b)) only these two areas have appeared to have distinct anomalies after compositing the several ENSO cycles. This may be interpreted as a teleconnection with some time lags. This teleconnection between the north Pacific and central Asia (or Eurasia) have not been noted in other previous studies except Chen (1982). He noted weak negative simultaneous correlation between the SOI and 700 mb height anomalies over central Asia, though the correlations of other areas are more significant (*e.g.*, north Pacific through the Atlantic). But once the time lag is taken to half a year or one year, this time-lag teleconnection seems to be dominated.

Another feature to be noted may be the eastward propagation of anomalous circulation from Eurasia toward the northern Pacific, though standing-type anomalies between the two areas seem to be more prominent. Interestingly, the eastward propagation of anomalous circulation along this latitude (40°–60°N) seems to be nearly synchronized with that of zonal wind along the equator as shown in Fig. 7. For example, the eastward propagation of cyclonic circulation at 200 mb (negative anomalies in Fig. 14 (a)) seems to be in phase with that of westerly anomalies at 200 mb along the equator (positive anomalies in Fig. 7 (a)). If so, the large negative anomalies

over north Pacific associated with El Niño events, which are noted as part of PNA pattern (Horel and Wallace, 1981), cannot be interpreted solely as a response of anomalous heating over the equatorial Pacific.

The overall features shown in Fig. 14 are not resulted from the 'time and space filtering' and 'composite' effects. To examine this, the longitude section of time-lag correlations of 500 mb geopotential height anomalies are computed along 40°–60°N. In this case only 11-month moving average is applied to height anomalies (from normal). Fig. 15 shows the result for the reference point over central Asia (60°E). The eastward movement of positive correlations with positive time lags (each point lags behind the reference point) from central Asia toward north Pacific is noted. In this case, the statistical significance level of 95% correspond with $\gamma = 0.2$. This correlation pattern implies that about one year after the positive (negative) anomalies appear over central Asia the anomalies of the same sign tend to appear over the north Pacific. Another feature to be noted may be that the north Pacific (120°E–180°) leads central Asia with 6 to 12 months lag with significant negative correlations. Nearly contemporaneous positive correlation between central Asia and 100°–120°W (around the Rockies) are also noticeable. Thus, the composite anomaly pattern as shown in Fig. 14 can fundamentally be reproduced in the lag-correlation diagram by using low-pass filtered 500 mb height anomalies.

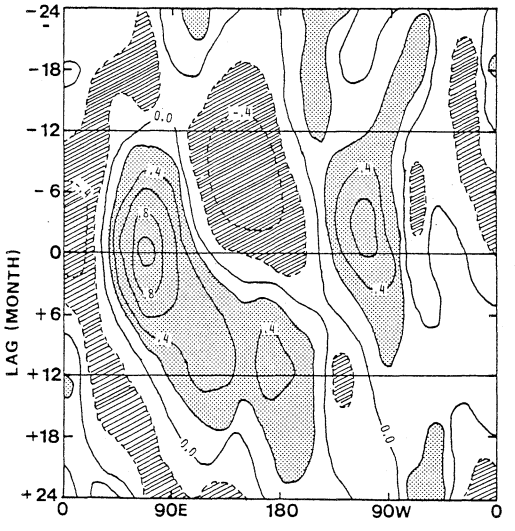

Fig. 15. Lag correlations of 500 mb geopotential height anomalies along 50°N with reference to 60°E. Units are 0.2. Positive values (>0.2) are hatched and negative values (<–0.2) are shaded.

The overall feature as noted in Fig. 14 (or Fig. 15) may be inferred as follows: the anti-cyclonic anomalies over north Pacific associated with anti-El Niño condition may cause cylonic and cold anomalies over central Asia after a half or one year. This anomalous circulation over central Asia may be responsible for more than normal snow cover extent, which further leads weak summer monsoon over India. The weak monsoon over India may be associated with weak tropical east-west circulation over the Indian Ocean through the equatorial Pacific, which may trigger the El Niño event *via* the weaking of the Pacific trades or the burst of equatorial westerlies over central Pacific. The anomalous circulation in the southern Indian Ocean through the southern Pacific may be involved in this process through some inter-hemispheric response of the southern westerlies to that in the northern hemisphere. This process along the equator may also be manifested as the eastward propagation of the anomalous east-west circulation along the equator as noted by Yasunari (1985) and others. Once the El Niño condition is established, the anticyclonic anomalies over north Pacific is changed to cyclonic anomalies, which in turn may lead the change of circulation anomalies over central Asia *via* the time-lag teleconnection mentioned above. The anti-cyclonic anomalies over central Asia may be favourable for strong summer monsoon over India, which in turn may intensify the tropical east-west circulation. Thus, anti-El Niño condition is again established *via* the circulation change over the north Pacific through Eurasia.

A big question may be, then, what is a physical mechanism of the 'time-lag teleconnection' between the north Pacific and central Asia. One possible mechanism may be a slow downstream amplification which is initiated as PNA (or anti-PNA) pattern over the north Pacific through the north Atlantic by anomalous heating over the equatorial Pacific, which finally causes the large amplification of anomalies over Eurasia. The downstream anomaly pattern from the north Pacific certainly seems to show some kind of

wave train with slight time lags. Reiter (1982) also suggested similar mechanism. However, some problems may arise such as why only the anomalies over central Asia are so amplified, even though central Asia is located at the most downstream side from the north Pacific.

Another possibility may be more direct coupling of these two areas *via* some land-atmosphere-ocean interaction. For example, the warm SST anomalies in the north Pacific and the north Atlantic during anti-El Niño phase (refer to Fig. 6 of Part I) may set up the warm troposphere along mid-latitudes (30°N–70°N). This feature is clearly demonstrated in the 300 mb temperature anomaly field at categories 1, 2 and 3 (Fig. 10). This warm condition in the middle latitudes implies the more zonal westerly flow (*i.e.*, high-index circulation) at high latitudes associated with the shrinkage of the cold polar vortex toward the arctic region. Under this condition, the thermal contrast between the warm oceans and the continents may be seasonally strongly intensified during winter when the continents are cooled. In response to this thermal contrast, anomalous ridge and trough may be intensified over the oceans and the continents, respectively. Particularly over Eurasia, where the cooling effect may be far stronger than that over north America, this anomalous trough seemingly forms a real stationary trough with the cold air mass over the interior of Eurasia. In fact, the long-term Eurasian pattern (Blackmon *et al.*, 1984) with negative height anomalies over Eurasia seems to correspond well to this anomalous circulation pattern in the northern winter. Very recently, Morinaga and Yasunari (1986) has found that this Eurasian pattern is greatly responsible for the large-extent of snow cover over central Asia. The snow cover may further strengthen the land-ocean thermal contrast. However, if this condition develops and persists even in the beginning of warmer seasons, it may weaken the following summer monsoon most probably *via* snow cover effect, which in turn weakens the east-west circulation along the tropics. The El Niño condition may be, thus, triggered following the process as mentioned earlier.

6. Conclusion

Time evolutions of anomalies of SST and atmospheric parameters over the global domain were investigated for the several ENSO cycles during the period from 1964 to 1979 by using objectively analyzed time-filtered data sets. These anomalies were subjected to composite technique relevant to each phase of the ENSO cycle as well as simple time sectional analysis along longitudes and latitudes. The evolution of the anomalies from anti-El Niño to El Niño and *vice versa* were described and summarized as a scenario of the quasi-periodic global climate system including oceanic and land-surface process. Some plausible physical mechanisms of this system were also discussed. The principal results are summarized as follows;

1) The eastward propagation of SLP and zonal wind field from the Indian Ocean toward the eastern Pacific is a fundamental nature of ENSO along the equator and the southern subtropics. Although SO has been traditionally understood as a standing oscillation of SLP between the Indian Ocean and the eastern Pacific, this propagating feature may also be an important facet of ENSO.
2) The significant anomalies of SLP and circulation field which first appear over the Indian Ocean seem to originate from central Asia or Eurasia. The vertical combination of SLP, temperature and streamfunction anomalies suggest that these anomalies over central Eurasia at the intermediate stages (category 3 and 7) are related to cold (or warm) air outbreak with more (or less) snow cover anomalies there. The structure of SLP evolution presented here has substantiated the evidences of global ENSO previously shown by Barnett (1985) and Krishnamurti *et al.* (1986).
3) A time-lag teleconnection between the north Pacific and central Asia was found in the circulation anomalies, which seems to have a dominant role on the ENSO cycle, namely the phase change from anti-El Ninño to El Niño and *vice versa*.

The links among the tropical and the extra-tropical oceans, and the Eurasian continent described above lead us to the idea that ENSO

should be considered to be a land-atmosphere-ocean coupled system as a whole rather than a plain atmosphere-ocean coupled system over the equatorial Pacific. In this system, the Asian summer monsoon seems to play an important role as a connector of oceanic process and land process. In this context, Normand's viewpoint (Normand, 1953) on the monsoon/SO relation that "The Indian monsoon stands out as an active, not a passive feature in world weather, more efficient as a broadcasting tool than as an event to be forecast" should be reevaluated.

Some critical problems are still remained for future studies. One problem may be the physical mechanism of the time-lag teleconnection as described here. In the present study, the ENSO cycles were examined for the near-periodic phase (1964–79) with a periodicity of 3 to 4 years. However, the ENSO also has considerable variances in aperiodic and non-stationary portions in the long-term period. This problem also deserves to be studied as an interaction of climate systems among different time scales. Another problem may be a more exact assessment of the role of the southern hemisphere on ENSO, which could not be made sufficiently because of the quality of the data sets. This may be one of the important subjects for the forthcoming TOGA.

Acknowledgements

The author is greatly indebted to Prof. T.N. Krishnamurti for his great support, encouragement and stimulating discussions throughout the work. The research reported here is mainly supported by NOAA Grant No. NA85AA-H CA019. The research is partly supported by Grant-In-Aid for 1985 (No. 26) from the Toray Science Foundation, and by the project research at the University of Tsukuba.

References

Arkin, P.A., 1982: The relationship between interannual variability in the 200 mb tropical wind field and the Southern Oscillation. *Mon. Wea. Rev.*, **110**, 1393–1404.

Barnett, T.P., 1984: Interaction of the monsoon and Pacific trade wind system at interannual time scales. Part III: A partial anatomy of the Southern Oscillation. *Mon. Wea. Rev.*, **112**, 2388–2400.

———, 1985a: Variations in near-global sea level pressure, *J. Atmos. Sci.*, **42**, 478–501.

———, 1985b: Three-dimensional structure of low frequency pressure variations in the tropical atmosphere. *J. Atmos. Sci.*, **42**, 2798–2803.

Bhalme, H.N. and S.K. Jadhav, 1984: The southern oscillation and its relation to the monsoon rainfall. *J. Climat.*, **4**, 509–520.

Blackmon, M.L., Y.-H. Lee and J.M. Wallace, 1984: Horizontal structure of 500 mb height fluctuations with long, intermediate and short time scales. *J. Atmos. Sci.*, **41**, 961–979.

Chen, W.Y., 1982: Fluctuations in Northern Hemisphere 700 mb height field associated with the Southern Oscillation. *Mon. Wea. Rev.*, **110**, 808–823.

Dey, B. and Bhanu Kumar, O.S.R.U., 1982: An apparent relationship between Eurasian spring snow cover and the advance period of the Indian summer monsoon. *J. App. Met.*, **21**, 1929–1933.

Dickson, R.R., 1984: Eurasian snow cover versus Indian summer monsoon rainfall– An extension of the Hahn–Shukla results. *J. App. Met.*, **23**, 171–173.

Gill, A.E., 1980: Some simple solutions for heat-induced tropical circulation. *Quart. J. Roy. Met. Soc.*, **106**, 447–462.

——— and E.M. Rassmusson, 1983: The 1982–83 climate anomaly in the equatorial Pacific. *Nature*, **306**, 229–234.

Gutzler, D.S. and D.E. Harrison, 1986: The structure and evolution of seasonal wind anomalies over the near-equatorial eastern Indian and western Pacific Oceans. Submitted to *Mon. Wea. Rev.*

Hahn, D.G. and J. Shukla, 1976: An apparent relationship between Eurasian snow cover and Indian summer monsoon rainfall. *J. Atmos. Sci.*, **33**, 2461–2462.

Horel, J.D. and J.M. Wallace, 1981: Planetary-scale atmospheric phenomena associated with the Southern Oscillation. *Mon. Wea. Rev.*, **109**, 813–829.

Hsiung, J. and R.E. Newell, 1983: The principal nonseasonal modes of variations of global sea surface temperature. *J. Phy. Oceangr.*, **13**, 1957–1967.

Kawamura, R., 1986: Seasonal dependency of atmosphere-ocean interaction over the north Pacific. *J. Met. Soc. Japan*, **64**, 363–371.

Kidson, J.W., 1975: Tropical eigenvector analysis and the Southern Oscillation. *Mon. Wea. Rev.*, **103**, 187–194.

Krishnamurti, T.N., S.H. Chu and W. Iglesias, 1986: On the sea level pressure of the Southern Oscillation. *Arch. Met. Geoph. Biocl.*, Ser. A, **34**, 385–425.

Luther, D.S., D.E. Harrison and R.A. Knox, 1983: Zonal winds in the central equatorial Pacific and El Niño. *Science*, **222**, 327–330.

Matsuno, T., 1966: Quasi-geostrophic motions in the equatorial area. *J. Met. Soc. Japan*, **44**, 25–43.

Morinaga, Y. and T. Yasunari, 1986: Interactions between the large-scale snow cover and the general circulation in the northern hemisphere. *Abstract of annual meeting of Japanese Soc. Snow and Ice*, 255. (in Japanese).

Newell, R.E., R. Selkirk and W. Ebisuzaki, 1982: The

Southern Oscillation: Sea surface temperature and wind relationships in a 100-year data set. *J. Climat.*, **2**, 357–373.

Niebauer, H.J., 1986: El Niño-Southern Oscillation teleconnections with the subarctic Bering Sea. Submitted to *J. Geophy. Res.*

Normand, C., 1953: Monsoon seasonal forecasting. *Quart. J. Roy. Met. Soc.*, **79**, 463–473.

Pan, H-L., 1979: Upper tropospheric tropical circulations during a recent decade. *Florida State University Report No.* 79–1. Department of Meteorology, FSU. 141pp.

Pan, Y-H. and A.H. Oort, 1983: Global climate variations connected with sea surface temperature anomalies in the eastern equatorial Pacific Ocean for the 1958–73 period. *Mon. Wea. Rev.*, **111**, 1244–1258.

Pant, G.B. and B. Parthasarathy, 1981: Some aspects of an association between the Southern Oscillation and Indian summer monsoon. *Arch. Met. Geoph. Biokl.*, Ser. B, **29**, 245–252.

Philander, S.G.H., T. Yamagata and R.C. Pacanowski, 1984: Unstable air-sea interactions in the tropics. *J. Atmos. Sci.*, **41**, 604–613.

Reiter, E.R., 1978: The interannual variability of the ocean-atmosphere system. *J. Atmos. Sci.*, **35**, 349–370.

————, 1982: Where we are and where we are going in mountain meteorology. *Bull. Ame. Met. Soc.*, **63**, 1114–1122.

————, 1983: Teleconnections with tropical precipitation surges. *J. Atmos. Sci.*, **40**, 1631–1647.

Rosen, R.D., D.A. Salstein, T.M. Eubanks, J.O. Dickey and J.A. Steppe, 1984: An El Niño signal in atmospheric angular momentum and earth rotation. *Science*, **225**, 411–414.

Shukla, J. and D.A. Paolino, 1983: The Southern Oscillation and long-range forecasting of the summer monsoon rainfall over India. *Mon. Wea. Rev.*, **111**, 1830–1837.

Troup, A.J., 1965: The 'Southern Oscillation'. *Quar. J. Roy. Met. Soc.*, **81**, 490–506.

van Loon, H. and D.J. Shea, 1985: The Southern Oscillation. Part IV: The precursors south of 15°S to the extremes of the oscillation. *Mon. Wea. Rev.*, **113**, 2063–2074.

———— and ————, 1987: The southern oscillation. Part VI: Anomalies of sea level pressure on the southern hemisphere and of Pacific sea surface temperature during the development of a warm event. In press in *Mon. Wea. Rev.*, **116**, January issue.

Walker, G.T. and E.W. Bliss, 1932: World weather V. *Mem. Roy. Met. Soc.*, **4**, 53–84.

Yamagata, T., Y. Shibao and S. Umatani, 1985: International variability of the Kuroshio Extension and its relation to the Southern Oscillation/El Niño. *J. Oceangr. Soc. Japan*, **41**, 274–281.

Yasunari, T., 1985: Zonally propagating modes of the global east-west circulation associated with the Southern Oscillation. *J. Met. Soc. Japan*, **63**, 1013–1029.

————, 1987: Global structure of El Niño/Southern Oscillation. Part I. El Niño composites. *J. Met. Soc. Japan*, **65**,

ＥＮＳＯ（エル・ニーニョ／南方振動）の全球構造 第２部：ＥＮＳＯサイクルに伴う変化

安 成 哲 三*

（フロリダ州立大学気象学教室）

第１部で記述されたデータにより，ＥＮＳＯサイクルに伴う海面水温及び大気構造の全球的な変化を解析し，以下のような結果が得られた。

1）熱帯および南半球亜熱帯では，地上気圧と大気循環のアノマリーに，インド洋上に出現し，東部太平洋上へと伝播する東進の位相が顕著である。

2）インド洋上に出現するこれらのアノマリーは，反対エル・ニーニョ期からエル・ニーニョ期（又はその逆）に移行する中間段階に，ユーラシア大陸上に現われるアノマリーと深い関連がある。ユーラシア大陸上でのアノマリーは，とくに下部対流圏で傾圧的な鉛直構造を示し，積雪分布のアノマリーとも対応していることから，インド洋方面への大規模な寒気吹き出しの強化（又は弱化）と対応していることが示唆される。

3）ユーラシア大陸上の大気循環のアノマリーと北太平洋上のアノマリーとの間に，時間のズレを持ったテレコネクションが認められる。このテレコネクションはＥＮＳＯサイクルにおいて，重要な役割を果していると推測される。

以上の結果は，ＥＮＳＯを全球的な大陸（雪氷）—大気—海洋相互作用として把えるべきことを示唆している。

* 現在所属：筑波大学地球科学系